

Correlation Effects on the Double Exchange Model in a Ferromagnetic Metallic Phase

Yoshiki IMAI and Norio KAWAKAMI

Department of Applied Physics, Osaka University, Suita, Osaka 565-0871

(Received)

The effect of the Hubbard interaction among conduction electrons on the double exchange model is investigated in a ferromagnetic metallic phase. Applying iterative perturbation theory to the Hubbard interaction within dynamical mean field theory, we calculate the one-particle spectral function and the optical conductivity, in which coherent-potential approximation is further used to treat the ferromagnetic Hund coupling between conduction electrons and localized spins. Identifying the decrease of the magnetization for the localized spin with the increase of the temperature, we discuss the temperature dependence of the one-particle spectrum and the optical conductivity. It is found that the interplay between the Hund coupling and the Hubbard interaction dramatically changes the spectral function, while it is somehow obscured in the optical conductivity.

KEYWORDS: correlated electron systems, double exchange model, iterative perturbation theory

§1. Introduction

There has been a resurgence of interest in doped perovskite manganese oxides such as $R_{1-x}A_x\text{MnO}_3$ (R is rare-earth and A is alkaline-earth ions), since the discovery of the colossal magnetoresistance. These compounds show a variety of interesting phenomena,^{1,2,3,4,5,6} which are caused by several competing interactions including not only spin but also charge and orbital degrees of freedom.^{7,8,9,10,11,13,15,16,17,18,19,20,12,14} Since the ferromagnetic state in a metallic phase is stabilized by the Hund coupling between localized spins and conduction electrons, the double exchange model has been used as a proper model to describe the ferromagnetic metallic manganites.^{7,8,9} Various unusual properties observed experimentally have been clarified by using this model, in which the Coulomb interaction among conduction electrons has been neglected for simplicity,^{9,10,11} or has been assumed to be infinitely strong.¹³ However, the finite Coulomb interaction should play an important role for the dynamics in Mn oxides, stimulating further theoretical studies to take into account the finite Hubbard interaction U , which have been done for the fully polarized case.^{15,16,17,18,19} More recently, Held and Vollhardt have studied the effect of the finite Hubbard interaction on a paramagnetic metallic phase by means of dynamical mean field theory (DMFT) and have claimed that such correlation effects indeed play an important role together with the Hund coupling.²⁰

In this paper, we study electron correlation effects on the double exchange model in a ferromagnetic metallic phase by introducing the finite Hubbard interaction among conduction electrons. The present study is based on the approach of Shiba et al.^{10,11} with coherent potential approximation (CPA), and is in some respects complementary to the work done by Held and Vollhardt for a paramagnetic phase.²⁰ By exploiting iterative per-

turbation theory (IPT) within DMFT for the Hubbard interaction, we compute the one-particle spectrum and the optical conductivity in which we further use CPA to deal with the Hund coupling. Based on the obtained results, we qualitatively discuss the temperature dependence of the above-mentioned dynamical quantities. It is shown that the introduction of the Hubbard interaction dramatically changes the one particle spectral function in the double exchange model. We also find that the optical conductivity is affected by the interplay of these two interactions, although it is not so conspicuous as in the one-particle spectrum.

§2. Iterative Perturbation Theory Approach

We study the double exchange model with the on-site Hubbard interaction in three dimensions. The Hamiltonian is given by

$$H = \sum_{\langle i,j \rangle \sigma} t_{ij} c_{i\sigma}^\dagger c_{j\sigma} - J \sum_i \boldsymbol{\sigma}_i \cdot \mathbf{S}_i + U \sum_i n_{i\uparrow} n_{i\downarrow}, \quad (1)$$

where $c_{i\sigma}^\dagger$ ($c_{i\sigma}$) is the creation (annihilation) operator of a conduction electron with the spin σ ($=\uparrow, \downarrow$) at the site i , and $n_{i\sigma} = c_{i\sigma}^\dagger c_{i\sigma}$. For simplicity, the orbital degeneracy is neglected in this paper. The Hund coupling J between a localized spin \mathbf{S}_i ($S = 1$) and a conduction electron ($\boldsymbol{\sigma}_i$ is the Pauli matrix) is assumed to be ferromagnetic.

We shall treat the electron correlations due to the Hubbard interaction within DMFT,²³ which is known as a powerful method to systematically study strongly correlated electron systems. The treatment with DMFT becomes exact in the limit of large spatial dimensions,^{21,22} and even for three dimensions, it provides a powerful method which has successfully described a number of important phenomena, such as the Mott transition, in strongly correlated electron systems.^{24,25,26} To perform the DMFT procedure, we further make use of IPT (see

below),^{24, 27, 28, 29, 30)} which correctly reproduces the self-energy both in the weak coupling limit as well as the atomic limit, and furthermore properly interpolates the two limiting cases.

We use CPA to treat the ferromagnetic Hund coupling. The validity of applying CPA to the double exchange model is summarized as follows.¹¹⁾ We are now dealing with the ferromagnetic Hund coupling, so that the dynamics of localized spins may be described rather well by that of classical spins, because the ferromagnetic order considerably suppresses quantum effects. It may be thus legitimate to replace the local spin \mathbf{S}_i by the classical Ising spin, and to further use CPA for treating Hund coupling for partially polarized ferromagnetic phase,¹¹⁾ in which random potentials are induced by thermal fluctuations of the Ising spins. Note that the CPA procedure is properly embedded in the self-consistent equations for DMFT,³¹⁾ because both methods are based on local approximations.

We carry out the following self-consistent procedure for IPT combined with CPA. Since the original lattice problem is converted to an effective single impurity problem in DMFT, let us first introduce the cavity Green function $\mathcal{G}_\sigma(\omega)$ and the dressed Green function $G_\sigma(\omega)$,

$$\mathcal{G}_\sigma(\omega) = [\omega + i\delta + \mu - \tilde{E}_{f\sigma} - \Delta_\sigma(\omega)]^{-1}, \quad (2)$$

$$G_\sigma(\omega) = [\mathcal{G}_\sigma^{-1}(\omega) - \Sigma_{U\sigma}(\omega)]^{-1}, \quad (3)$$

where μ and $\Delta_\sigma(\omega)$ are the chemical potential and the renormalized hybridization function, respectively. Here we have denoted the self energy due to the Hubbard interaction as $\Sigma_{U\sigma}$ and $\tilde{E}_{f\sigma} = E_f + U n_{\bar{\sigma}}$ where E_f is the impurity level in the reduced single-site problem. Using the cavity Green function, the second-order self-energy due to the Hubbard interaction is expressed in a usual form,

$$\begin{aligned} \Sigma_{U\sigma}^{(2)}(\omega) &= U^2 \int_{-\infty}^{\infty} d\epsilon_1 \int_{-\infty}^{\infty} d\epsilon_2 \int_{-\infty}^{\infty} d\epsilon_3 \\ &\times \rho_\sigma(\epsilon_1) \rho_{\bar{\sigma}}(\epsilon_2) \rho_\sigma(\epsilon_3) \\ &\times \frac{f(\epsilon_1) f(-\epsilon_2) f(\epsilon_3) + f(-\epsilon_1) f(\epsilon_2) f(-\epsilon_3)}{\omega + i\delta - \epsilon_1 + \epsilon_2 - \epsilon_3} \end{aligned} \quad (4)$$

with $\rho_\sigma(\epsilon) = -1/\pi \text{Im}(\mathcal{G}_\sigma(\epsilon))$, where $f(\epsilon)$ is the Fermi distribution function. For arbitrary filling, we improve the approximation by modifying the second-order self energy as,

$$\Sigma_{U\sigma}(\omega) = \frac{A_\sigma \Sigma_{U\sigma}^{(2)}(\omega)}{1 - B_\sigma \Sigma_{U\sigma}^{(2)}(\omega)} \quad (5)$$

with

$$A_\sigma = \frac{n_{\bar{\sigma}}(1 - n_{\bar{\sigma}})}{n_{0\bar{\sigma}}(1 - n_{0\bar{\sigma}})}, \quad B_\sigma = \frac{(1 - n_{\bar{\sigma}})U + E_f + \mu}{n_{0\bar{\sigma}}(1 - n_{0\bar{\sigma}})U^2} \quad (6)$$

where $n_{0\sigma}$ and n_σ are the particle numbers respectively defined by $n_{0\sigma} = -1/\pi \int_{-\infty}^{\infty} d\omega f(\omega) \text{Im}\mathcal{G}_\sigma(\omega)$ and $n_\sigma = -1/\pi \int_{-\infty}^{\infty} d\omega f(\omega) \text{Im}G_\sigma(\omega)$.^{29, 30)} Note that the coefficients A_σ and B_σ have been introduced so as to reproduce the correct results in the high energy limit and the atomic limit, respectively.

We now incorporate the effect of the Hund coupling by

introducing an additional self energy $\Sigma_{H\sigma}$, which enters in the local Green function as,

$$\begin{aligned} \tilde{G}_\sigma^{\text{loc}}(\omega) &= \frac{1}{N} \sum_k \tilde{G}_\sigma(k, \omega) \\ &= \int_{-\infty}^{\infty} d\epsilon \frac{N_0(\epsilon)}{\omega + i\delta - \epsilon + \mu - \tilde{E}_{f\sigma} - \Sigma_{U\sigma}(\omega) - \Sigma_{H\sigma}(\omega)}, \end{aligned} \quad (7)$$

where $\tilde{G}_\sigma(k, \omega)$ denotes the one-particle Green function in the lattice system. We employ the semielliptic form as the bare density of states, $N_0(\epsilon) = 2/(\pi D^2) \sqrt{D^2 - \epsilon^2}$ with the bandwidth D . Following a standard CPA procedure, the average of the random scattering of conduction electrons due to localized spins should be zero, leading to

$$\left\langle \frac{-JS_i\sigma - \Sigma_{H\sigma}(\omega)}{1 - \tilde{G}_\sigma^{\text{loc}}(\omega)(-JS_i\sigma - \Sigma_{H\sigma}(\omega))} \right\rangle_{S_i} = 0, \quad (8)$$

which is rewritten in terms of the magnetization M of localized spins as,

$$\begin{aligned} \tilde{G}_\sigma^{\text{loc}}(\omega) \Sigma_{H\sigma}(\omega) + \Sigma_{H\sigma}(\omega) \\ - \tilde{G}_\sigma^{\text{loc}}(\omega) (JS)^2 + \sigma JM = 0. \end{aligned} \quad (9)$$

The self-consistency condition requires the local Green function in Eq. (7) to be equivalent to the dressed impurity Green function in Eq. (3). We thus obtain,

$$\Delta_\sigma(\omega) = \frac{D^2}{4} \tilde{G}_\sigma^{\text{loc}}(\omega) + \Sigma_{H\sigma}(\omega). \quad (10)$$

Note that the chemical potential μ should be determined by the Friedel sum rule in the reduced impurity problem. This completes the description of our IPT approach combined with CPA.

§3. Correlation Effects on Dynamical Quantities

We have performed the numerical calculation by iterating the procedure mentioned in the previous section until each quantity should converge within a desired accuracy. The one-particle spectrum of conduction electrons thus computed is shown in Fig. 1. We first mention that since we are dealing with the dynamics of localized spins by CPA, the change in the magnetization may be approximately considered to be caused by thermal fluctuations.¹¹⁾ Namely, the magnetization of localized spins M is increased from (a) to (d), which implies in our treatment that the temperature is monotonically decreased from $T = T_C$ (critical temperature) down to $T = 0$.

We start our discussions with the case of (a), where there is no magnetization in the system. In this paramagnetic phase, the spectrum near the Fermi surface in the $U = 2$ case gets narrower than the non-interacting case. In addition to this band-narrowing effect, there is the life-time effect, which is accompanied by a small structure developed around the energy for the doubly occupied state. These aspects are in agreement with those obtained by Held and Vollhardt.²⁰⁾ With the increase of M (decrease of the temperature), the spectral function

shows quite different behaviors for up- and down-spin electrons. The spectral function for up-spin electrons is gradually reduced to the original semielliptic form, whereas that for down-spin electrons starts to develop several hump structures, whose origin will be discussed below momentarily. Note also in (b) that the spectrum with up- (down-) spin electrons in the $U = 2$ case shifts to a lower (higher) energy side compared with the noninteracting case, which is caused by the interplay between the Hubbard and the Hund interactions. Namely, since the magnetic susceptibility of conduction electrons is enhanced by the Hubbard interaction, the magnetization of conduction electrons for a given M of localized spins becomes larger for larger U via the Hund coupling, giving rise to the large self-energy shift observed in (b). We will see below that this shift affects the profile of the optical conductivity. For reference, we show the magnetization of conduction electrons as a function of M for several choices of U in Fig. 2.

As M is further increased, the spectral function for down-spin electrons develops three distinct peaks (Fig. 1(c)). To see the origin of the structure, we first recall that conduction electrons in (c) are almost fully polarized, though localized spins are still partially polarized ($M = 0.8$), as a consequence of the enhanced spin susceptibility (see Fig. 2). Thus adding a down-spin electron to an unoccupied site may have two possibilities depending on whether the corresponding localized spin is parallel or antiparallel to the spin of the added electron. The former contributes to the lowest-energy peak where the added electron gains the energy $-J$, while the latter forms the middle peak with the energy increment J for making antiparallel spins. On the other hand, if a down-spin electron is added to the site already occupied by an up-spin electron, this makes the highest-energy peak in the spectrum. Note that the position of the lowest-energy peak is pushed from the bare level up to slightly above the Fermi level, which is again caused by the self-energy shift due to the Hubbard interaction and the Hund-coupling. To clearly show how the above three-peak structure is developed with the increase of the Hubbard interaction U , we display of $M = 0.8$ for several choices of U in Fig. 3. It is seen that the above-mentioned three-peak structure is gradually formed with the increase of U , which is accompanied by the rather large self energy shift. Finally, in the case of (d), the localized spins are almost fully polarized, so that the spectrum for up-spin electrons is reduced to the non-interacting one, while the spectrum for down spin electrons still has the two-peak structure. As mentioned above, the lower peak represents a particle-addition spectrum to an empty site, while the upper peak corresponds to that for a singly occupied site. In all the cases (a)~(d), the interplay between the Hund coupling and the Hubbard interaction is important to determine the temperature dependence in the profile of the one-particle spectral function.

Experimentally, several nontrivial effects on the photoemission spectrum have been reported in the manganese compounds,^{34,35,36} which may not be simply explained without the Coulomb interaction. A typical example is that the band width observed in a paramagnetic

phase is about twice as large as that expected from the band calculation. This may be caused by the correlation effects among conduction electrons, as recently explained by Held and Vollhardt with the use of DMFT.²⁰ Our results in Fig. 1(a) are consistent with theirs as well as the experimental tendency. Also, it has been reported that the coherent spectrum near the Fermi surface is increased as the temperature is decreased below the critical temperature, indicating the decrease of effective electron correlations at low temperatures.^{34,35,36} Such effects are indeed seen in the present results of Fig. 1 for electrons with up spin, namely, the decrease of the temperature gradually reduces the effective interaction among conduction electrons in the filled band, being consistent with the experiments. Although our treatment here neglects several important effects due to the orbitally degenerate bands with anisotropic hoppings, etc, it turns out that some qualitative features obtained are consistent with those observed in the photoemission spectrum.

In order to further investigate the dynamical response in the system, we calculate the optical conductivity. We employ the following formula for the optical conductivity in which the vertex correction is neglected,

$$\begin{aligned} \sigma(\omega) &= \pi \sum_{\sigma} \int_{-\infty}^{\infty} d\epsilon' \int_{-\infty}^{\infty} d\epsilon \\ &\times N_0(\epsilon) A_{\sigma}(\epsilon, \epsilon') A_{\sigma}(\epsilon, \omega + \epsilon') \frac{f(\epsilon') - f(\epsilon' + \omega)}{\omega}, \quad (11) \\ A_{\sigma}(\epsilon, \omega) &= -\frac{1}{\pi} \\ &\times \text{Im} \left(\frac{1}{\omega + i\delta - \epsilon + \mu - \tilde{E}_{f\sigma} - \Sigma_{U\sigma}(\omega) - \Sigma_{H\sigma}(\omega)} \right). \quad (12) \end{aligned}$$

Note that this expression becomes exact in the limit of large dimensions.^{22,33,32} The computed results are shown in Fig. 4. As well known, the optical conductivity consists of two peaks, each of which corresponds to the Drude-like part and the interband part for which two separated bands are formed by the Hund coupling. Comparing the $U = 2$ case with the non-interacting one, we can see that the structure near the $\omega \sim 0$ (Drude-like peak) gets somewhat narrower via the correlation effect due to the Hubbard interaction. Also, we find that the hump structure corresponding to the interband excitations are smeared by the life-time effect due to the Hubbard interaction U , and this effect becomes more conspicuous when U is large, being consistent with the results deduced for a paramagnetic phase.²⁰ It should be noticed here that the maximum position of the interband excitations in the $U = 2$ case shows a non-monotonic behavior with the increase of the magnetization M , which is not observed in the noninteracting case. Namely, the maximum position in the $U = 2$ case is once lowered with the increase of the magnetization ($M = 0.5$), and then increased again up to the original position ($M = 0.8$). This is a consequence of the self energy shift induced by the Hubbard interaction and the Hund coupling: As mentioned in Fig. 1(b), the one-particle spectrum for $U = 2$ suffers from the large self-energy shift when M

is increased. If M is further increased, the self energy shift becomes small again, as seen in Fig. 1(c), (d), giving rise to the non-monotonic behavior of the interband excitations as a function of M . If the Hubbard interaction is further increased, the spectral weight of the interband excitations becomes small. In this way, the interplay of the Hubbard interaction and the Hund coupling appears in the optical conductivity, although it is somewhat obscured in contrast to a dramatic change in the one-particle spectrum.

§4. Summary

We have studied how the correlation effect among conduction electrons affects dynamical properties of the double exchange model in a ferromagnetic metallic phase. In order to investigate dynamical quantities in the whole energy region, we have exploited iterative perturbation theory combined with coherent potential approximation for the Hund coupling. By approximately relating the decrease of the magnetization of the localized spin with the increase of the temperature, we have discussed the temperature dependence of the one-particle spectrum and the optical conductivity. It has been shown that the interplay between the Hund coupling and the Hubbard interaction dramatically affects the profile of the one-particle spectrum, which results in a characteristic structure quite different from the non-interacting case. Some results have been found to be qualitatively consistent with photoemission experiments. On the other hand, the effect of the Hubbard interaction is somewhat smeared in the optical conductivity, although it indeed affects the profile for both of the Drude-like intraband part as well as the interband part.

We have shown that there appears a non-monotonic temperature dependence in the one-particle spectrum as well as the optical conductivity in a ferromagnetic phase, which is caused by the self-energy shift due to the Hubbard interaction and the Hund coupling. For example, such a behavior emerges in the interband excitations in the optical conductivity in Fig. 4. As already pointed out, however, the interband peak-structure is smeared when the Hubbard interaction is increased, presumably making it rather difficult to observe such a non-monotonic behavior. It seems thus interesting to check whether this type of the correlation effect could be observed experimentally in the one-particle density of states around the Fermi level.

In this paper, we have neglected the orbital degeneracy for conduction electrons as well as the corresponding off-diagonal components for the hopping matrix. Correlation effects including the orbital degrees of freedom may be expected to provide further nontrivial properties. To this end, it is necessary to extend the present study to such orbitally degenerate cases in a ferromagnetic phase.

Acknowledgements

We would like to thank S. Kumada and N. Furukawa for valuable discussions. The work is partly supported by a Grant-in-Aid from the Ministry of Education, Science, Sports, and Culture.

-
- [1] Y. Tokura, A. Urushibara, Y. Moritomo, T. Arima, A. Asamitsu, G. Kido and N. Furukawa: *J. Phys. Soc. Jpn.* **63** (1994) 3931
 - [2] A. Urushibara, Y. Moritomo, T. Arima, A. Asamitsu, G. Kido and Y. Tokura: *Phys. Rev. B* **51** (1995) 14103
 - [3] A. Asamitsu, Y. Moritomo, R. Kumai, Y. Tomioka and Y. Tokura: *Phys. Rev. B* **54** (1996) 1716
 - [4] Y. Okimoto, T. Katsufuji, T. Ishikawa, A. Urushibara, T. Arima and Y. Tokura: *Phys. Rev. Lett.* **75** (1995) 109
 - [5] Y. Okimoto, T. Katsufuji, T. Ishikawa, T. Arima and Y. Tokura: *Phys. Rev. B* **55** (1997) 4206
 - [6] A. P. Ramirez: *J. Phys.: Condens. Matter* **9** (1997) 8171
 - [7] C. Zener: *Phys. Rev.* **82** (1951) 403
 - [8] P. W. Anderson and H. Hasegawa: *Phys. Rev.* **100** (1955) 362
 - [9] N. Furukawa: *J. Phys. Soc. Jpn.* **63** (1994) 3214; **64** (1995) 2734; **64** (1995) 3164
 - [10] H. Shiba, R. Shiina and A. Takahashi: *J. Phys. Soc. Jpn.* **66** (1997) 941
 - [11] P. E. Brito and H. Shiba: *Phys. Rev. B* **57** (1998) 1539
 - [12] S. Ishihara, J. Inoue and S. Maekawa: *Phys. Rev. B* **55** (1997) 8280
 - [13] S. Ishihara, M. Yamanaka and N. Nagaosa: *Phys. Rev. B* **56** (1997) 686
 - [14] R. Maezono, S. Ishihara and N. Nagaosa; *Phys. Rev. B* **57**, 13993 (1998); **58**, 11583 (1998)
 - [15] H. Nakano, Y. Motome and M. Imada: *J. Phys. Soc. Jpn.* **68** (1999) 2178
 - [16] Y. Motome and M. Imada: *Phys. Rev. B* **60** (1999) 7921
 - [17] P. Horsch, J. Jaklic and F. Mack: *Phys. Rev. B* **59** (1999) 6217
 - [18] R. Kilian and G. Khaliullin: *Phys. Rev. B* **58** (1998) 11841; G. Khaliullin and R. Kilian: *Phys. Rev. B* **61** (2000) 3494
 - [19] V. Ferrari and M. J. Rozenberg: *cond-mat/9906131*
 - [20] K. Held and D. Vollhardt: *cond-mat/9909311*, to appear in *Phys. Rev. Lett.*
 - [21] W. Metzner and D. Vollhardt: *Phys. Rev. Lett.* **62** (1989) 324
 - [22] E. Müller-Hartmann: *Z. Phys. B* **74** (1989) 507; **76** (1989) 211
 - [23] A. George, G. Kotliar, W. Krauth and M. J. Rozenberg: *Rev. Mod. Phys.* **68** (1996) 13
 - [24] X. Y. Zhang, M. J. Rozenberg and G. Kotliar: *Phys. Rev. Lett.* **70** (1993) 1666
 - [25] M. Jarrel and T. Pruschke: *Z. Phys. B* **90** (1993) 187; *Phys. Rev. B* **49** (1993) 1458
 - [26] M. Jarrell, H. Akhlaghour and T. Pruschke: *Quantum Monte Carlo Methods in Condensed Matter Physics*, edited by M. Suzuki (World Scientific, 1993)
 - [27] A. George and G. Kotliar: *Phys. Rev. B* **45** (1992) 6479
 - [28] M. J. Rozenberg, G. Kotliar and X. Y. Zhang: *Phys. Rev. B* **49** (1994) 10181
 - [29] H. Kajueter and G. Kotliar: *Phys. Rev. Lett.* **77** (1996) 131
 - [30] T. Saso: *J. Phys. Soc. Jpn.* **68** (1999) 3941
 - [31] M. S. Laad, L. Craco and E. Müller-Hartmann: *cond-mat/9911378*
 - [32] A. Khurana: *Phys. Rev. Lett.* **64** (1990) 1990
 - [33] T. Pruschke, D. L. Cox and M. Jarrel: *Phys. Rev. B* **47** (1993) 3553
 - [34] D. D. Sarma, N. Shanthi, S. R. Krishnakumar, T. Saitoh, T. Mizokawa, A. Sekiyama, K. Kobayashi, A. Fujimari, E. Weschke, R. Meier, G. Kaindl, Y. Takeda and M. Takano: *Phys. Rev. B* **53** (1996) 6873
 - [35] J. -H. Park, C. T. Chen, S. -W. Cheong, W. Bao, G. Meigs, V. Chakarian and Y. U. Idzerda: *Phys. Rev. Lett.* **76** (1996) 4215
 - [36] T. Saitoh, A. Sekiyama, K. Kobayashi, T. Mizokawa, A. Fujimari, D. D. Sarma, Y. Takeda and M. Takano: *Phys. Rev. B* **56** (1997) 8836

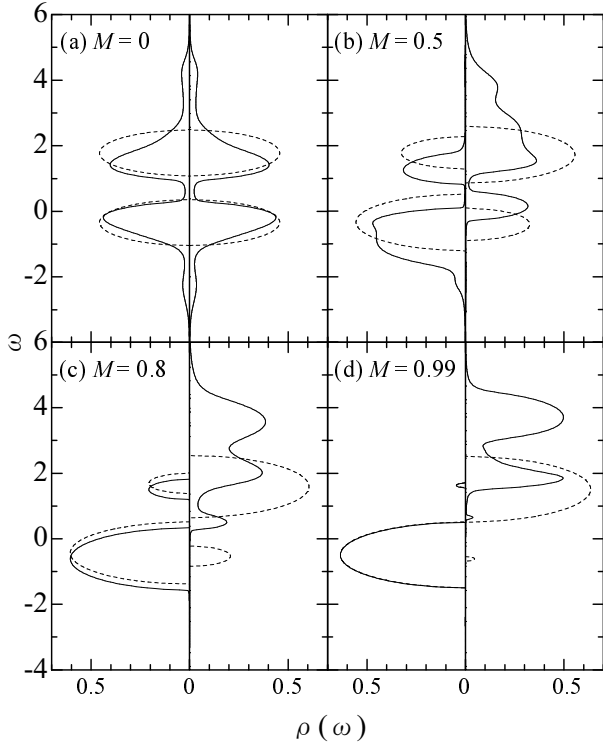


Fig. 1. One-particle spectral function $\rho(\omega)$ calculated by IPT and CPA; (a) $M = 0$ (Curie temperature), (b) $M = 0.5$, (c) $M = 0.8$, (d) $M = 0.99$ ($T \sim 0\text{K}$). The hole (electron) concentration is $x = 0.2$ (0.8). In all figures, the left (right) panel represents the spectrum for up (down) spin electrons. The energy is measured from the Fermi level $\omega = 0$, and the bandwidth D is taken to be unity. The Hund coupling is taken as $J = 1$, and the Hubbard interaction is set to be $U = 2$ (solid line) and $U = 0$ (dashed line).

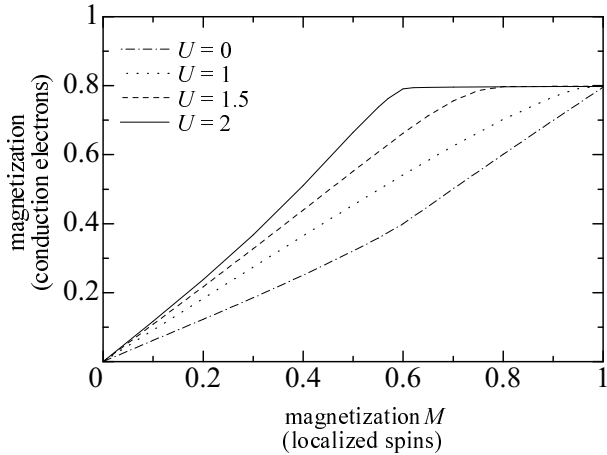


Fig. 2. Plot of the magnetization for conduction electrons as a function of that for localized spins M for various U . The hole concentration is $x = 0.2$. The other parameters are as in Fig. 1.

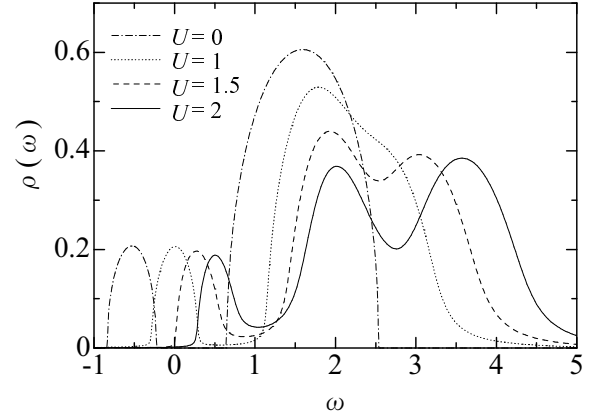


Fig. 3. One-particle spectral function $\rho(\omega)$ for down spin electrons for various U in the case of $M = 0.8$. The other parameters are as in Fig. 1.

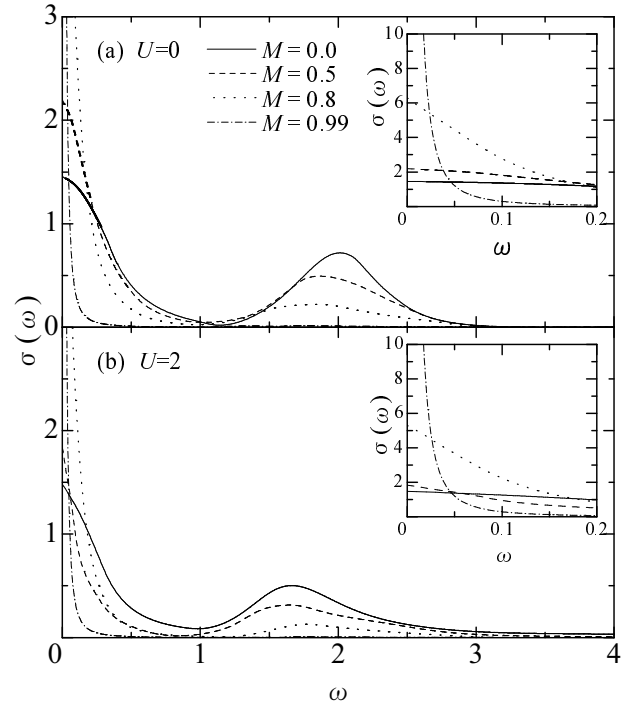


Fig. 4. Optical conductivity $\sigma(\omega)$ for (a) $U = 0$, (b) $U = 2$; $M = 0$ (solid), $M = 0.5$ (dashed), $M = 0.8$ (dotted) and $M = 0.99$ (dash-dotted), respectively. The insets show the low-frequency part. The other parameters are as in Fig. 1.